Trap and Carrier Transport of Pristine and Aged Silicone Rubber by Surface Potential Measurements

Wenbin Kang[1], Chenyu Yan[2], Shijun Li[2], Yin Huang[2], Daomin Min[2*], and Shengtao Li[2]
[1] China Electric Power Research Insutitute, Wuhan, 430074, China
[2] State Key Laboratory of Electrical Insulation and Power Equipment, Xi'an Jiaotong University, Xi'an, 710049, China
*E-mail: forrestmin@mail.xjtu.edu.cn

***Abstract*—Silicone rubber is widely used in power equipment such as cable joint. In order to get better performance of insulator, it is significant to evaluate the insulation condition of aged silicone rubber insulators. Thus in this paper, surface potential decay measurement has been applied to investigate the performance of pristine and aged silicone rubber. Pristine and aged silicone rubber samples are charged by positive and negative corona discharging. Then the surface potentials are measured by a non-contact probe. It is found that surface potential in aged rubber decays faster, which is resulted from more shallow traps generated during ageing process, for electrons are easier to migrate or even trap out of the shallow traps. Additionally, carrier mobility shows an increase in aged rubber for both positive and negative charges, which may be resulted from the increase in shallow traps in the material. As regards to conductivity, it turns out that conductivity in aged rubber is higher than that in pristine one, which indicates charges in aged rubber migrate faster and further proves the conclusion mentioned that shallow traps increase in internal material.**

Keywords: Ageing, carrier transport, silicone rubber, surface potential decay, trap density

I. INTRODUCTION

Silicon rubber composite insulator is widely used in the electric power transmission system all over the world. Compared with porcelain and glass insulators, silicone rubber insulators show good performance with lower pollution [1-3]. However, during long-time work, charges are easily generated on the surface of material, which may lead to flashover and further affect the performance of electric equipment [4-6]. In this regard, it is significant to investigate the generated charge to evaluate the aged degree of material.

In recent few decades, many researchers focus on the mechanism of surface charge generation, distribution and its impact on flashover, whereas a specific explanation has not been approached. Kindersberger analyzes the approaches of charge decay and conduct simulation of experimental analysis of surface charge accumulation and decay for silicone rubber, epoxy resin and tetrafluoroethylene ring [7-9]. Kumada pays attention to the algorithm of surface charge, transferring the relation of charge density and probe response in electrostatic probe method from spatial domain to spatial frequency domain, which effectively accelerate the calculation [10]. Min et.al investigate the influence of electron beam irradiation on surface trap properties and surface conduction of epoxy resin microcomposites [11].

Supported by the National Natural Science Foundation of China (NSFC) under Project with No. 51337008, the National Basic Research Program of China (973 Program) under Project with No. 2015CB251003, and NSFC under Projects with Nos. 51323012 and 51221005. It was also supported by State Key Laboratory of Power System of Tsinghua University (SKLD16KZ04).

II. EXPERIMENTAL PREPARATION AND PROCESS

A. Samples

A silicone rubber sample with a thickness of about 2.0 mm was aged ac voltage of 10 kV with 5, 7, 11 and 13 harmonic components for 30 days. A pristine silicone rubber sample was used for control experiments. Both samples are paved and stuck on the copper plate.

B. Experimental process

Prior to introducing the process, experimental method and equipment will be introduced here. Fig. 1 illustrates the structure of surface potential decay measurement system. This system is a typical needle-grid electrode system, consisting high voltage needle electrode, metal grid electrode and grounding electrode system. During the experiment, higher voltage is applied to the needle electrode, while lower voltage is applied to the grid electrode, thus needle will appear corona discharge and generate lots of charges, then charges will migrate to the surface of sample under the effect of electric field. During the experiment, the sample will firstly be charged by applied voltage and then moved right below the probe, which will detect the potential on the surface and transfer data to the computer, where Labview is applied to collect the data and generate Excel sheet.

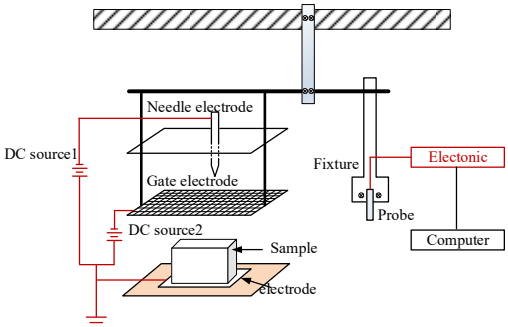

Figure 1. Surface potential decay measurement system.

In this paper, two groups of experiments were conducted.

(1) Negative corona charging

Pristine sample: needle electrode voltage is -10 kV, grid electrode voltage is -5 kV, period of charging is 2 min, detection period is 9 h.

Aged sample: needle electrode voltage is -10 kV, grid electrode voltage is -5 kV, period of charging is 2min, detection period is 4 h.

(2) Positive corona charging

Pristine sample: needle electrode voltage is 10 kV, grid electrode voltage is 5 kV, period of charging is 2 min, detection period is 9 h.

Aged sample: needle electrode voltage is 10 kV, grid electrode voltage is 5 kV, period of charging is 2 min, detection period is 4 h.

III. Experiment Results and Analysis

A. Experimental results

During the experiment, probe detects the surface potential once a second, Excel sheet can be transferred to image to demonstrate the potential decay tendency and results are shown as Fig. 2.

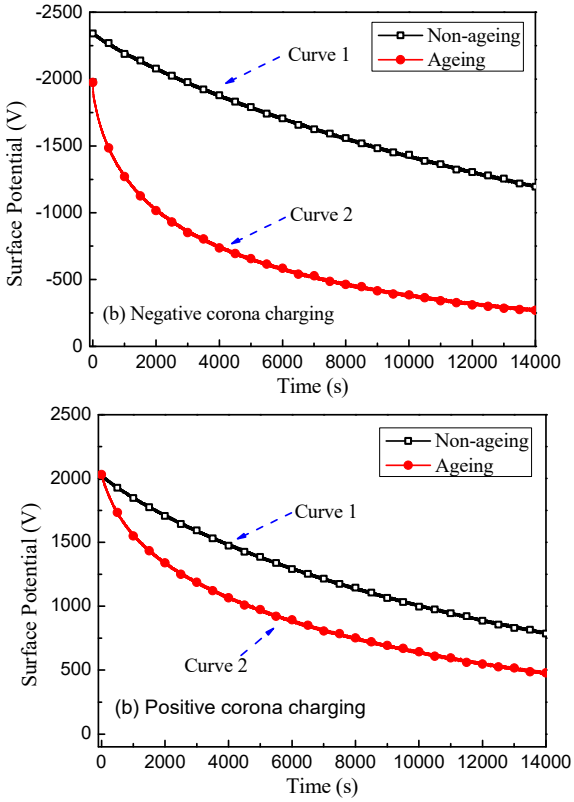

Figure 2. Surface potential decay curves of pristine and aged SiR samples after (a) negative corona charging and (b) positive corona charging.

As Fig. 2 indicates, under both of negative and positive corona, ageing sample shows a faster decay rate than the pristine one, which manifests more shallow traps are generated during ageing. Additionally, it needs to be noticed that for aging sample, the curve drops more remarkably under the negative corona than that under the positive corona, thus it can be deduced that hole traps are deeper than electron traps, leading to fast decrease of surface potential. Moreover, compared with two curves in a) and b), samples under negative corona reach a higher potential than that under the positive corona, which further prove the previous conclusion that hole traps are more than electron traps.

B. Trap distribution analysis

It is agreed that potential decay is closely relating to the distribution of traps. Fig. 3 shows the potential decay process caused by detrapping of charges from surface traps.

In accordance with the surface potential decay theory, raised by Simmons [12, 13], it can be obtained the surface trap energy level in function of surface trap density as equation

$$E_{ST} = \kappa_B T In\left(\nu_{ATE} t\right), \tag{1}$$

where E_{ST} represents surface trap energy level in eV; κ_B is Boltzmann constant, equaling to 1.38×10^{-23} J/K; T is absolute temperature in K; ν_{ATE} is attempt-to-escape frequency in s^{-1}; Additionally, attempt-to-escape frequency can be expressed as $\kappa_B T/h$, where h is Planck constant, equaling to 6.63×10^{-34} Js.

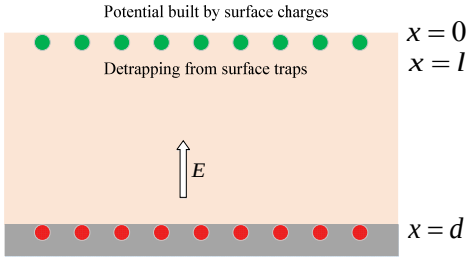

Figure 3. Schematic of surface potential decay model caused by detrapping of charges from surface traps.

In addition, surface trap density in function of potential decay rate can be obtained by equation

$$N_{trap}\left(E_{ST}\right) = \frac{\varepsilon_0 \varepsilon_r}{edL} t \frac{\partial \phi_s(t)}{\partial t} \tag{2}$$

where d is thickness of sample in m; $\phi_s(t)$ is surface potential in V. for simplification, $\partial\phi_s(t)/\partial t$ can be fitted in accordance with

$$\phi_s = \phi_s(0) + A_1 \exp\left(-x/t_1\right) + A_2 \exp\left(-x/t_2\right) \tag{3}$$

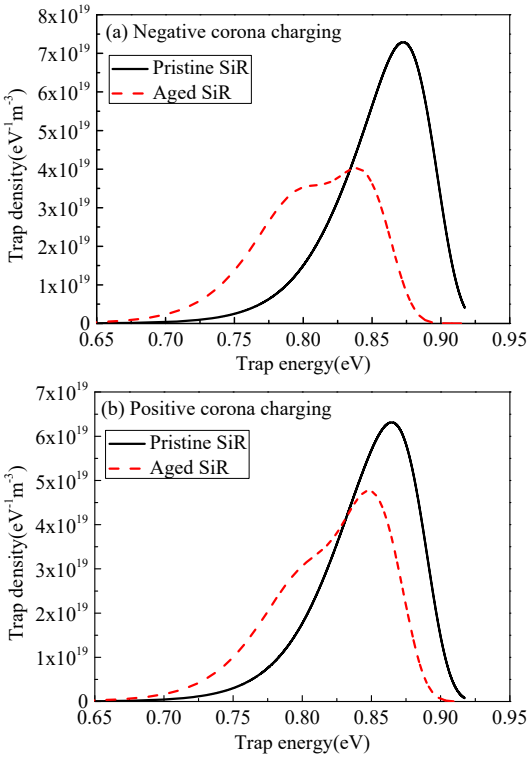

Figure 4. Surface trap distributions for pristine and aged SiR samples after (a) negative corona charging and (b) positive corona charging.

Fig. 4 manifests the trap density in function of trap energy. It can be obtained that trap energies in both samples under positive and negative corona decrease, energy of deep trap is

around 0.87 eV for pristine sample but that in ageing sample decreases to around 0.85 eV, while energy of shallow declines to 0.78 eV or so. Additionally, shallow trap amount get larger and deep trap amount decline. In this way, electrons in shallow traps are easier to trap out and shift away, resulting potential decay, thus process of potential decay in aged rubber conducts faster than non-age one. As regards to the reason why shallow trap amount rise up, it may be resulted from long-time exposure and work and specific mechanism still remains to be investigated.

C. *Carrier mobility analysis*

Surface potential decay measurement results also indicate the regulation of carrier mobility, which can be estimated from the initial surface potential decay rate by [14, 15],

$$-\left(\frac{\mathrm{d}\phi_s}{\mathrm{d}t}\right)_{t=0}=\frac{\mu}{2}\left(\frac{\phi_s}{d}\right)^2_{t=0}. \tag{4}$$

Additionally, surface potentials and corresponding decay rates can also be used for estimating carrier mobility, which can be visually viewed. Here carrier mobilities estimated with equation (4) and initial surface potentials and corresponding decay rates are estimated from the experimental curves are shown in Table 1 and Fig. 5 respectively.

TABLE I. CARRIER MOBILITES OF POSITIVE AND NEGATIVE CHARGES ESTIMATED BY EQUATION (4).

SiR sample	Carrier mobility of positive charges ($m^2V^{-1}s^{-1}$)	Carrier mobility of negative charges ($m^2V^{-1}s^{-1}$)
Pristine	2.6×10^{-13}	1.0×10^{-13}
Aged	6.1×10^{-12}	1.5×10^{-12}

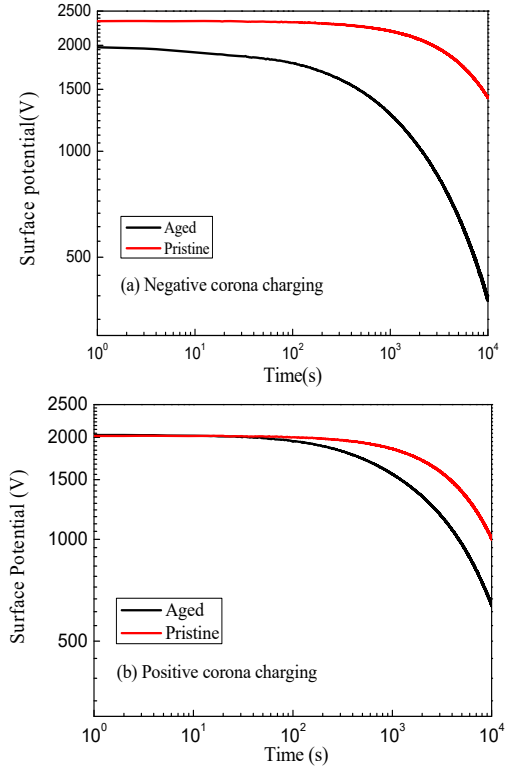

Figure 5. Surface potential as a function of decay time in logarithmic coordinates after (a) negative corona charging and (b) positive corona charging.

It is noticeable that a transition point exists in each figure, which is represented by transit time t_t. Carrier mobility then can be estimated by the following equation.

$$\mu=\frac{d^2}{\phi_s t_t} \tag{5}$$

In this way, carrier mobilities of positive and negative charges are presented in Table 2.

TABLE II. CARRIER MOBILITES OF POSITIVE AND NEGATIVE CHARGES ESTIMATED BY EQUATION (5).

SiR sample	Carrier mobility of positive charges ($m^2V^{-1}s^{-1}$)	Carrier mobility of negative charges ($m^2V^{-1}s^{-1}$)
Pristine	3.2×10^{-13}	1.8×10^{-13}
Aged	5.5×10^{-12}	1.7×10^{-12}

It can be seen that two columns of data are relatively close, which is also an indication that results are valid for analysis. It is easy to find that carrier mobility aged silicone rubber is higher than that in pristine one, consequently, higher carrier mobility results in higher decay rate in aged rubber, which is in good agreement with experimental results.

D. *Conductivity*

It is reasonable to estimate conductivity through Surface potential decay results, for conductivity itself is a parameter of demonstrating charge transportation in material bulk. Conductivity in function of potential decay obeys [16],

$$\frac{\mathrm{d}\phi_s}{\mathrm{d}t}=-\frac{\phi_s(t)\gamma(\phi_s)}{\varepsilon_0\varepsilon_r} \tag{6}$$

where $\gamma(\phi_s)$ is intrinsic conductivity of sample, including electronic conductivity and hole conductivity.

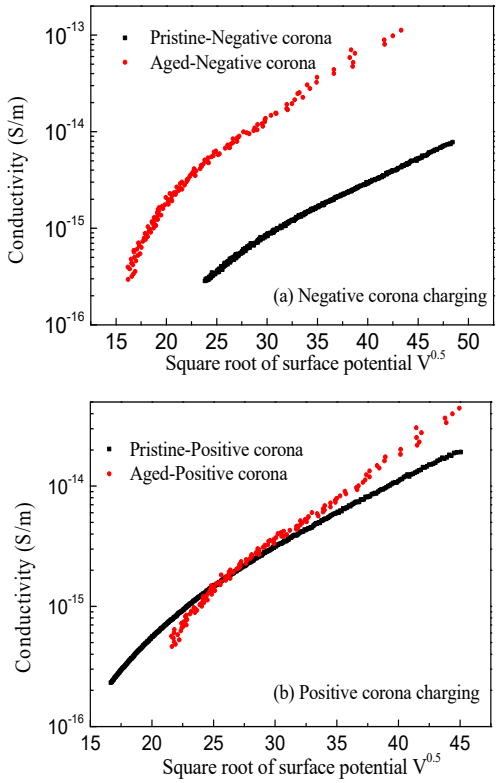

Figure 6. Conductivity as a function of square root of surface potential. (a) negative corona charging, (b) positive corona charging

In addition, derived value can be compared with different models of field dependent conductivity, such as Poole-Frenkel model (PF) [16, 17]

$$\gamma(\phi_s) = \gamma_0 \exp\left(\frac{e\sqrt{e\phi_s/d\pi\varepsilon_0\varepsilon_r}}{\kappa_B T}\right). \quad (7)$$

In equation (7), γ is considered to be a factor in function of $\sqrt{\phi_s}$. Conductivity as a function of square root surface potential are drawn in Fig. 6. It can be obviously seen that conductivity decreases with a decrease in surface potential, which is resulted by decrease in built-in electric field. Additionally, it turns out that conductivity in aged silicone rubber is higher than that in pristine one, which indicates charges in aged rubber migrate faster and further proves the conclusion mentioned that shallow traps increase in material.

IV. Conclusion

Surface potential decay characters have been tested and analyzed. Conclusions of the paper are shown below.

(1) Surface potential decays faster in aged silicone rubber than that in the pristine one.

(2) More hole traps than electron ones exist in both aged and pristine material.

(3) More shallow traps appear in the aged silicone rubber compared with pristine one, which allow electrons migrate easier.

(4) Carrier mobilities for positive and negative charges are higher in aged silicone rubber than those in pristine one.

(5) Conductivity decreases with a decrease in surface potential, and it turns out that conductivity in aged rubber is higher than that in pristine one.

Reference

[1] N. Allen, A. Hashem, H. Rodrigo and B. Tan. "Streamer development on silicone-rubber insulator surfaces", IEE Proceedings-Science, Measurement and Technology, Vol. 151, 31-38, 2004.

[2] S. Jun, Z. Yaoming and Y. Chongling. "Properties of silicone rubber insulators and their applications in high voltage", High Voltage Apparatus, Vol. 45, 155-158, 2009.

[3] Z. Liu. "Electric power and energy in China", 2012 (in Chinese).

[4] Q. Wang, G. Zhang and X. Wang. "Characteristics and mechanisms of surface charge accumulation on a cone-type insulator under DC voltage", IEEE Transactions on Dielectrics and Electrical Insulation, Vol. 19, 2012.

[5] R. Wilkins. "Flashover voltage of high-voltage insulators with uniform surface-pollution films", Proceedings of the Institution of Electrical Engineers, Vol. 116, 457-465, 2010.

[6] Y. Liang, Z. Jin and J. Zhang. "Influence of Surface Charge on Surface Flashover of Silicone Rubber at Different Corona Aging Time", Proceedings of The Chinese Society for Electrical Engineering, Vol. 36, 2016 (in Chinese).

[7] J. Kindersberger and C. Lederle. "Surface charge decay on insulators in air and sulfurhexafluorid-Part I: Simulation", IEEE Transactions on Dielectrics and Electrical Insulation, Vol. 15, 941-948, 2008.

[8] J. Kindersberger and C. Lederle. "Surface charge decay on insulators in air and sulfurhexafluorid-Part II: Measurements", IEEE Transactions on Dielectrics and Electrical Insulation, Vol. 15, 949-957, 2008.

[9] A. Winter and J. Kindersberger. "Stationary resistive field distribution along epoxy resin insulators in air under DC voltage", IEEE Transactions on Dielectrics and Electrical Insulation, Vol. 19, 2012.

[10] A. Kumada, S. Okabe and K. Hidaka. "Resolution and signal processing technique of surface charge density measurement with electrostatic probe", IEEE Transactions on Dielectrics and Electrical Insulation, Vol. 11, 122-129, 2004.

[11] L. Shengjun, H. Yin, M. Daomin, L. Zhen, X. Dongri, L. Shengtao, Z. Chong and X. Zhaoliang. "Effect of electron beam irradiation on surface trap characteristics and surface conductivity of epoxy micro composites", Insulation Material, Vol. 49, 55-61, 2016 (in Chinese).

[12] J. Simmons, G. Taylor and M. Tam. "Thermally stimulated currents in semiconductors and insulators having arbitrary trap distributions", Physical Review B, Vol. 7, 3714, 1973.

[13] J. Simmons and M. Tam. "Theory of isothermal currents and the direct determination of trap parameters in semiconductors and insulators containing arbitrary trap distributions", Physical Review B, Vol. 7, 3706, 1973.

[14] T. Mizutani and M. Ieda. "Carrier transport in high-density polyethylene", Journal of Physics D: Applied Physics, Vol. 12, 291, 1979.

[15] M. M. Perlman, T. J. Sonnonstine and J. A. St. Pierre. "Drift mobility determinations using surface‐potential decay in insulators", Journal of Applied Physics, Vol. 47, 5016-5021, 1976.

[16] R. Coelho, B. Aladenize, N. Cornet and J. Bigarre. "On the transient potential in insulators", IEEE Transactions on Dielectrics and Electrical Insulation, Vol. 8, 760-770, 2001.

[17] J. Frenkel. "On Pre-Breakdown Phenomena in Insulators and Electronic Semi-Conductors", Physical Review, Vol. 54, 647-648, 1938.